

# Hole and Electron Extraction Layers Based on Graphene Oxide Derivatives for High-Performance Bulk Heterojunction Solar Cells

Jun Liu, Yuhua Xue, Yunxiang Gao, Dingshan Yu, Michael Durstock, and Liming Dai\*

Graphene, having a single-atom-thick sheet of carbon atoms packed in a 2D honeycomb lattices,<sup>[1,2]</sup> possesses excellent electronic, thermal, and mechanical properties attractive for a large variety of potential applications, including transparent electrodes and/or active materials in electronic devices, solar cells, supercapacitors, batteries, fuel cells, actuators, and sensors.<sup>[3–9]</sup> Graphene has also been found to be useful as the platform of biomedical sensors.<sup>[10]</sup> The recent availability of solution-processable graphene by exfoliation of graphite into graphene oxides (GOs), followed by solution reduction, has allowed the functionalization, characterization, and processing of graphene sheets via various solution methods. It has been demonstrated that GO consists of epoxy and hydroxyl groups on the basal plane and carboxylic groups at the edge.<sup>[11,12]</sup> The C–O bonds on the basal plane disrupt the conjugation of the hexagonal graphene lattice to render GO insulator or semiconductor. Due to strong interactions between the hexagonally sp<sup>2</sup>-bonded carbon layers in graphite, the solution oxidation of graphite requires strong oxidizing reagents (e.g., HNO<sub>3</sub>, KMnO<sub>4</sub>, and/or H<sub>2</sub>SO<sub>4</sub>) under harsh conditions.<sup>[13]</sup> This often leads to severe damage to the carbon basal plane, and hence a poorly defined electronic structure. It remains a big challenge to design GO-based materials with controlled electronic properties for high-performance device applications. Further to our work on functionalization of graphene (oxide),<sup>[13–15]</sup> we have recently found that simple charge neutralization of the –COOH groups in GO with Cs<sub>2</sub>CO<sub>3</sub> could tune the electronic structure of GO,

making GO derivatives useful as both hole- and electron-extraction layers in bulk heterojunction (BHJ) solar cells.

BHJ solar cells with a layer of electron donor/acceptor (e.g., poly(3-hexylthiophene) (P3HT):[6,6]-phenyl-C<sub>61</sub>-butyric acid methyl ester (PCBM)) blend forming a bicontinuous network between cathode and anode have recently received great attention due to their relatively high energy-conversion efficiency and low production cost.<sup>[16–30]</sup> Under operation, the two electrodes with different work functions create an internal built-in field to facilitate holes to transport towards and be collected on the high work function electrode (anode) while electrons to transport towards and be collected on the low work function electrode (cathode). For high-performance solar cells, work functions of the cathode and the anode need to match the LUMO level of the acceptor and the HOMO level of the donor, respectively, to reduce energy barriers for electron- and hole-extraction. The energy barriers between the active layer and electrodes can often be effectively reduced by electron-/hole-extraction layers at the cathode/anode (see **Figure 1**).<sup>[20,21]</sup> Examples of the hole-extraction layer includes conductive polymers (e.g., poly(styrenesulfonate) doped poly(3,4-ethylenedioxythiophene), PEDOT:PSS),<sup>[20]</sup> self-assembled organic molecules,<sup>[22]</sup> and vacuum deposited inorganic metal oxide layer (e.g., MoO<sub>3</sub>, V<sub>2</sub>O<sub>5</sub>, NiO).<sup>[23,24]</sup> On the other hand, certain metal fluorides,<sup>[20]</sup> n-type semiconductors (e.g., TiO<sub>2</sub>, TiO<sub>x</sub>, ZnO),<sup>[25,26]</sup> n-type organic semiconductors (e.g., 2,9-dimethyl-4,7-diphenyl-1,10-phenanthroline, BCP),<sup>[27]</sup> and conjugated polymer electrolytes<sup>[28]</sup> have been used as the electron extraction layer. The work function of a hole-extraction material should be relatively high to allow for the built-in electrical field across the active layer and for holes to transport towards the anode. Similarly, an electron extraction layer needs to have a low work function for electrons to efficiently transport to the cathode. To our best knowledge, no single material system has been demonstrated to serve as both hole-extraction layer and electron-extraction layer due to the stringent requirement on the work function. If realized, the single hole-/electron-extraction material system could not only simplify the materials design and device fabrication but also allow for a precise control of the energy barrier for electron- and hole-extraction by tuning its work function via, for example, controlled functionalization.

Herein, we report our recent finding on functionalization of GO to produce both hole- and electron-extraction materials for BHJ solar cells. **Scheme 1** shows the chemical structures of the hole-extraction GO and the electron-extraction Cesium-neutralized GO (GO–Cs), in which the periphery –COOH groups in GO were replaced by –COOCs groups through

Dr. J. Liu, Dr. Y. Xue, Dr. Y. Gao, Dr. D. Yu, Prof. L. Dai  
Center of Advanced Science and Engineering  
for Carbon (Case4Carbon)  
Department of Macromolecular  
Science and Engineering  
Case School of Engineering  
Case Western Reserve University  
10900 Euclid Avenue, Cleveland, Ohio 44106, USA  
E-mail: liming.dai@case.edu



Dr. Y. Xue  
Institute of Advanced Materials for Nano-Bio Applications  
School of Ophthalmology & Optometry  
Wenzhou Medical College  
Zhejiang 325027, China  
Dr. M. Durstock  
Materials and Manufacturing Directorate  
Air Force Research Laboratory, RXBP  
Wright-Patterson Air Force Base  
Ohio 45433, USA

DOI: 10.1002/adma.201104945

Report Documentation Page				Form Approved OMB No. 0704-0188	
Public reporting burden for the collection of information is estimated to average 1 hour per response, including the time for reviewing instructions, searching existing data sources, gathering and maintaining the data needed, and completing and reviewing the collection of information. Send comments regarding this burden estimate or any other aspect of this collection of information, including suggestions for reducing this burden, to Washington Headquarters Services, Directorate for Information Operations and Reports, 1215 Jefferson Davis Highway, Suite 1204, Arlington VA 22202-4302. Respondents should be aware that notwithstanding any other provision of law, no person shall be subject to a penalty for failing to comply with a collection of information if it does not display a currently valid OMB control number.					
1. REPORT DATE <b>2012</b>		2. REPORT TYPE		3. DATES COVERED <b>00-00-2012 to 00-00-2012</b>	
4. TITLE AND SUBTITLE <b>Hole and Electron Extraction Layers Based on Graphene Oxide Derivatives for High-Performance Bulk Heterojunction Solar Cells</b>				5a. CONTRACT NUMBER	
				5b. GRANT NUMBER	
				5c. PROGRAM ELEMENT NUMBER	
6. AUTHOR(S)				5d. PROJECT NUMBER	
				5e. TASK NUMBER	
				5f. WORK UNIT NUMBER	
7. PERFORMING ORGANIZATION NAME(S) AND ADDRESS(ES) <b>Case Western Reserve University, Center of Advanced Science and Engineering for Carbon (Case4Carbon), 10900 Euclid Avenue, Cleveland, OH, 44106</b>				8. PERFORMING ORGANIZATION REPORT NUMBER	
9. SPONSORING/MONITORING AGENCY NAME(S) AND ADDRESS(ES)				10. SPONSOR/MONITOR'S ACRONYM(S)	
				11. SPONSOR/MONITOR'S REPORT NUMBER(S)	
12. DISTRIBUTION/AVAILABILITY STATEMENT <b>Approved for public release; distribution unlimited</b>					
13. SUPPLEMENTARY NOTES					
14. ABSTRACT					
15. SUBJECT TERMS					
16. SECURITY CLASSIFICATION OF:			17. LIMITATION OF ABSTRACT <b>Same as Report (SAR)</b>	18. NUMBER OF PAGES <b>6</b>	19a. NAME OF RESPONSIBLE PERSON
a. REPORT <b>unclassified</b>	b. ABSTRACT <b>unclassified</b>	c. THIS PAGE <b>unclassified</b>			

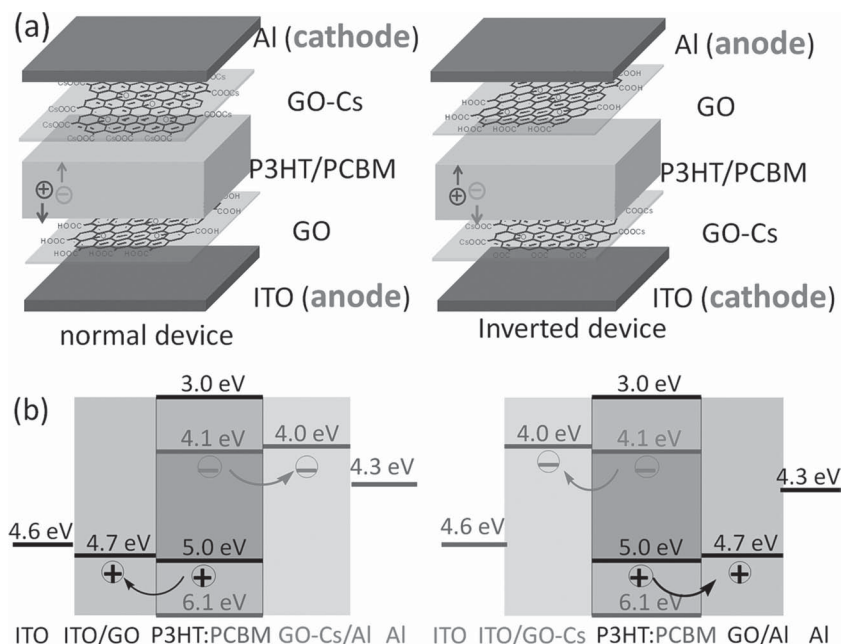
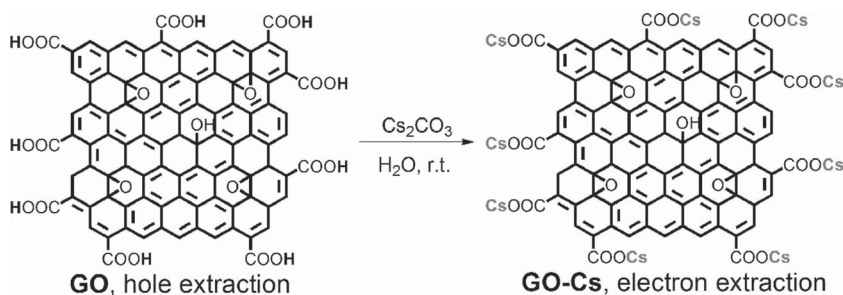


**Figure 1.** Device structures (a) and energy level diagrams (b) of the normal device and the inverted device with GO as hole-extraction layer and GO-Cs as the electron-extraction layer.

charge neutralization. GO itself has the work function of 4.7 eV, which matches the HOMO level of P3HT for hole extraction (see Figure 1). Moreover, the periphery  $\text{-COOH}$  groups in GO can dope P3HT of the active layer at the interface to facilitate an Ohmic contact for hole extraction. By replacing the periphery  $\text{-COOH}$  groups with the  $\text{-COOCs}$  groups through charge neutralization (Scheme 1), the work function of the GO-Cs modified Al can be reduced to 4.0 eV, which matches the LUMO level of PCBM for efficient electron-extraction (see Figure 1). Thus, the controlled functionalization demonstrated here renders GO derivatives to be the first single electron-/hole-extraction material system, which could open avenues to the design and development of novel electron-/hole-extraction materials from carbon and many other materials. As we shall see later, their charge-extraction performance is fairly comparable to those of the state-of-art hole- and electron-extraction materials currently used in BHJ solar cells. The relatively weak light absorption characteristic of GO and GO-Cs, together with their good solution-processability for ultrathin film formation (ca. 2 nm, vide infra), facilitates light transmission to the active layer



**Scheme 1.** Chemical structures and synthetic route of GO and GO-Cs.

for further improved device performance. Graphene thin films synthesized by chemical vapor deposition (CVD) have recently been proved to be efficient hole- and electron-collecting electrodes in BHJ solar cells<sup>[31,32]</sup> while BHJ solar cells with all-carbon active layer have also been demonstrated.<sup>[33]</sup> Therefore, our present work on the GO/GO-Cs hole-/electron-extraction materials, coupled with these earlier publications, holds promise for developing all-carbon flexible solar cells.

In a typical experiment, GO was synthesized according to the modified Hummer's method.<sup>[13]</sup> The  $\text{-COOH}$  groups of GO were neutralized with  $\text{Cs}_2\text{CO}_3$  in an aqueous solution to readily afford GO-Cs (Scheme 1). GO-Cs was then thoroughly purified by repeatedly dissolving in water and filtration through 0.2  $\mu\text{m}$  polyvinylidene fluoride (PVDF) membrane. The neutralization was confirmed by the pH value of 0.1  $\text{mg mL}^{-1}$  aqueous solution of GO (pH = 4.34) and GO-Cs (pH = 8.39). The resulting GO and GO-Cs were characterized by X-ray photoemission spectroscopy (XPS), atomic force microscopy (AFM), Raman spectroscopy, Fourier-transform infrared (FTIR) spectroscopy, X-ray diffraction (XRD), and thermogravimetric analysis (TGA).

**Figure 2a,b** show typical AFM images of GO and GO-Cs spin-coated from 0.5  $\text{mg mL}^{-1}$  aqueous solution on Si substrates. We can clearly observe individual single layer graphene oxide sheets with thickness of about 1 nm and lateral dimension of several hundred nanometers. No particle was observed in the AFM image of GO-Cs, implying the absence of residual  $\text{Cs}_2\text{CO}_3$ . The content of  $\text{Cs}^+$  in GO-Cs was estimated to be 6.7 mol% from the XPS spectra (Figure 2c). Figure S1 (Supporting Information, SI) shows the high-resolution C1s spectra for GO and GO-Cs. The relative intensity of C-O and COOH bands decreased upon addition of  $\text{Cs}_2\text{CO}_3$  to form GO-Cs. Similar spectroscopic changes had been observed by neutralizing GO with KOH.<sup>[34]</sup> The nearly identical Raman spectra of GO-Cs and GO (SI, Figure S2) indicate that the introduction of  $\text{Cs}^+$  did not cause much change of carbon skeletons in the graphene oxide basal plane due to the edge-functionalization. As reflected by the disappearance of the XRD diffraction peak (SI, Figure S4), however, the introduction of  $\text{Cs}^+$  into the semicrystalline GO solid turned it into amorphous.

This is because the ionic interaction of  $\text{-COO}^-$  and  $\text{Cs}^+$  during the functionalization of GO overwhelmed the  $\pi$ - $\pi$  interaction of graphene plane and caused further exfoliation of GO into individual graphene sheets in GO-Cs. The bandgap of GO and GO-Cs were estimated to be 2.74 eV and 1.79 eV, respectively, from their UV-vis absorption spectra (SI, Figure S5).

The device fabrication and characterization details are provided in the Experimental Section. For all the devices using GO and GO-Cs, the thickness of the GO layer and

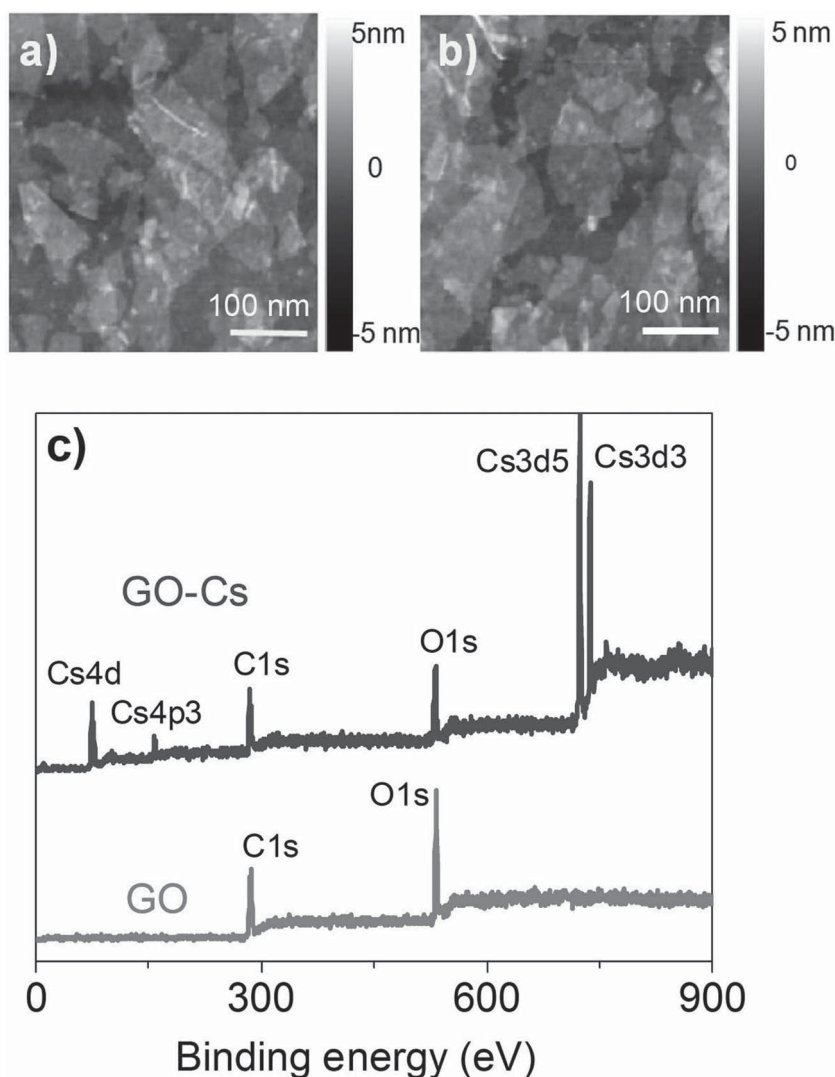


**Figure 2.** AFM images of a) GO and b) GO-Cs on silicon substrates. c) XPS profiles of GO and GO-Cs.

the GO-Cs layer are both fixed to be about 2 nm. The reference polymer solar cell has the configuration of indium tin oxide (ITO)/PEDOT:PSS/P3HT:PCBM/LiF/Al, in which the PEDOT:PSS is the hole-extraction layer and LiF is the electron-extraction layer, P3HT/PCBM blend is the active layer, ITO acts as anode and Al acts as the cathode.

To investigate the hole-extraction ability of GO, we compared three devices (device A, B, C in Table 1) with the same active layer (P3HT:PCBM), cathode (Al), electron-extracting layer (LiF), and anode (ITO), but with no (device A), PEDOT:PSS (device B) and GO (device C) as the hole-extraction layer. The current density–voltage curves ( $J$ – $V$ ) of these devices under simulated AM1.5G illumination at  $100 \text{ mW cm}^{-2}$  are shown in Figure 3a while the corresponding open-circuit voltage ( $V_{\text{OC}}$ ), short circuit-current density ( $J_{\text{SC}}$ ), fill factor (FF) and power-conversion efficiency (PCE) are listed in Table 1. The device A without a hole-extraction layer shows a very limited photovoltaic efficiency. In contrast, device B and device C with

hole-extraction layer exhibit much improved device performance with respect to device A. Moreover, device B and C also show much reduced dark current than that of device A (SI, Figure S8). The GO-based device C performs slightly better than PEDOT:PSS-based device B, implying that GO is an excellent hole-extraction material for BHJ solar cells.

To evaluate the ability of GO-Cs as the electron-extraction layer, we fabricated four devices (device B, D, E, F in Table 1) with the same anode (ITO), hole-extraction layer (PEDOT:PSS), active layer (P3HT:PCBM), and cathode (Al), but with no (device D), LiF (device B),  $\text{Cs}_2\text{CO}_3$  (device E), and GO-Cs (device F) as the electron-extraction layer. Comparing with device D without electron-extraction layer (Figure 3b, SI, Figure S8b and Table 1), the reference device B with the LiF layer shows similar  $J_{\text{SC}}$  and FF, but higher  $V_{\text{OC}}$  and PCE, as well as lower dark current, indicating the important role of the electron-extraction layer. In consistency with previously reported results,<sup>[35]</sup> the  $\text{Cs}_2\text{CO}_3$ -based device E exhibits slightly lower  $J_{\text{SC}}$  and PCE than those of the reference device B. The device based on GO-Cs as the electron-extraction layer (device F) exhibits fairly comparable  $V_{\text{OC}}$ ,  $J_{\text{SC}}$ , FF, and PCE with the reference device B based on LiF. These results clearly show the great capability of GO-Cs as electron-extraction material in BHJ solar cells.

The great hole-/electron-extraction capability of GO/GO-Cs are mainly attributable to their work functions. The work functions of GO and GO-Cs on Al, as measured by Kelvin probe force microscopy (KFM), are 4.6–4.8 eV and 3.9–4.1 eV, respectively. The observed work function difference is due to possible intramolecular charge-transfer from Cesium to GO component in GO-Cs, which reduces the work function. Besides, Cesium salts, such as  $\text{Cs}_2\text{CO}_3$  and  $\text{CsF}$ , have been reported to lower work function of Al cathode due to the formation of Cs–O–Al structure.<sup>[35,36]</sup> Similar Cs–O–Al structure formation may also work for GO-Cs. Because of the work function match between GO-Cs and the LUMO level of PCBM, GO-Cs modified electrode can form an Ohmic contact with the P3HT:PCBM active layer for efficient electron extraction. On the other hand, the work function of GO matches the HOMO level of P3HT to form an Ohmic contact with the P3HT:PCBM layer for efficient hole extraction. As proposed by Jen et al.,<sup>[37–39]</sup> GO with acidic COOH groups could dope P3HT at their interface to facilitate the Ohmic contact formation. The newly appeared long wavelength absorption band (650–900 nm) in the absorption spectra of GO/P3HT bilayer (SI, Figure S7) seems to support the interfacial doping in the present work. In addition to the above work function consideration, a low resistance of charge extraction layer is also important for good



**Table 1.** Device structures and performance of the BHJ solar cells studied.

No.	Device structure	$V_{OC}$ [V]	$J_{SC}$ [mA/cm <sup>2</sup> ]	FF	PCE [%]
A	ITO/P3HT:PCBM/LiF/Al	0.31	4.85	0.29	0.45
B	ITO/PEDOT:PSS/P3HT:PCBM/LiF/Al	0.61	9.67	0.52	3.15
C	ITO/GO/P3HT:PCBM/LiF/Al	0.64	10.15	0.50	3.25
D	ITO/PEDOT:PSS/P3HT:PCBM/Al	0.43	9.59	0.50	2.09
E	ITO/PEDOT:PSS/P3HT:PCBM/Cs <sub>2</sub> CO <sub>3</sub> /Al	0.62	7.81	0.53	2.58
F	ITO/PEDOT:PSS/P3HT:PCBM/GOCs/Al	0.62	9.81	0.50	3.08
G	ITO/GO/P3HT:PCBM/GOCs/Al	0.61	10.30	0.59	3.67
H	ITO/Cs <sub>2</sub> CO <sub>3</sub> /P3HT:PCBM/PEDOT:PSS/Al	0.42	6.03	0.47	1.20
I	ITO/GOCs/P3HT:PCBM/GO/Al	0.51	10.69	0.54	2.97

device performance. The basal plane of graphene oxide has been reported to be ambipolar and can transport both electrons and holes.<sup>[40]</sup> The conductivity of GO and GO-Cs, as measured by a four-probe method, are  $3.8 \times 10^{-3} \text{ S m}^{-1}$  and  $5.0 \times 10^{-3} \text{ S m}^{-1}$ , respectively. Table S1 (SI) lists the work function and conductivity of electron-/hole-extraction materials used in this study. We believe that the ambipolar characteristics intrinsically associated with the graphene oxide basal plane is another advantage for the application of graphene oxide derivatives as both hole and electron extraction layers.

The excellent hole-/electron-extraction capabilities demonstrated above for GO/GO-Cs prompted us to construct BHJ solar cells with both GO and GO-Cs. For this purpose, both the normal device with the configuration of ITO(anode)/GO/P3HT:PCBM/GO-Cs/Al(cathode) (device **G**, Table 1) and inverted device with the configuration of ITO(cathode)/GO-Cs/P3HT:PCBM/GO/Al(anode) (device **I**, Table 1) were investigated. Figure 1 shows the device structures and the energy level diagrams. Figure 3c depicts the  $J$ - $V$  curve for the device **G** and Table 1 lists the corresponding characteristics, which shows a  $V_{OC}$  of 0.61 V,  $J_{SC}$  of  $10.30 \text{ mA cm}^{-2}$ , FF of 0.59 and

PCE of 3.67%. The observed performance for device **G** is even better than that of the reference device **B** with the state-of-the-art PEDOT:PSS and LiF interlayers, indicating that GO and GO-Cs can work well in a single device. Recently, inverted solar cells with bottom transparent ITO as cathode have received particular attention because of their potential long lifetime at ambient conditions.<sup>[29,30]</sup> In the inverted device **I**, ITO is adjacent to the GO-Cs layer to act as the cathode for collecting electrons while Al is close to the GO layer and behaviors as the anode to collect holes. The  $J$ - $V$  curve of the device **I** is shown in Figure 3d and the corresponding characteristics are listed in Table 1. It gives a  $V_{OC}$  of 0.51 V,  $J_{SC}$  of  $10.69 \text{ mA cm}^{-2}$ , FF of 0.54, and PCE of 2.97%. Thus, device **I** showed a much better performance than that of the control inverted device **H** with Cs<sub>2</sub>CO<sub>3</sub> electron-extraction layer and PEDOT:PSS hole-extraction layer. For these two devices with both GO and GO-Cs, the inverted device **I** exhibited a lower  $V_{OC}$ , and hence a lower PCE than that of the normal device **G**. The observed good performance with high maximum external quantum efficiency (EQE) of 68% (SI, Figure S9) for both the normal and inverted devices containing GO and GO-Cs indicate that the charge

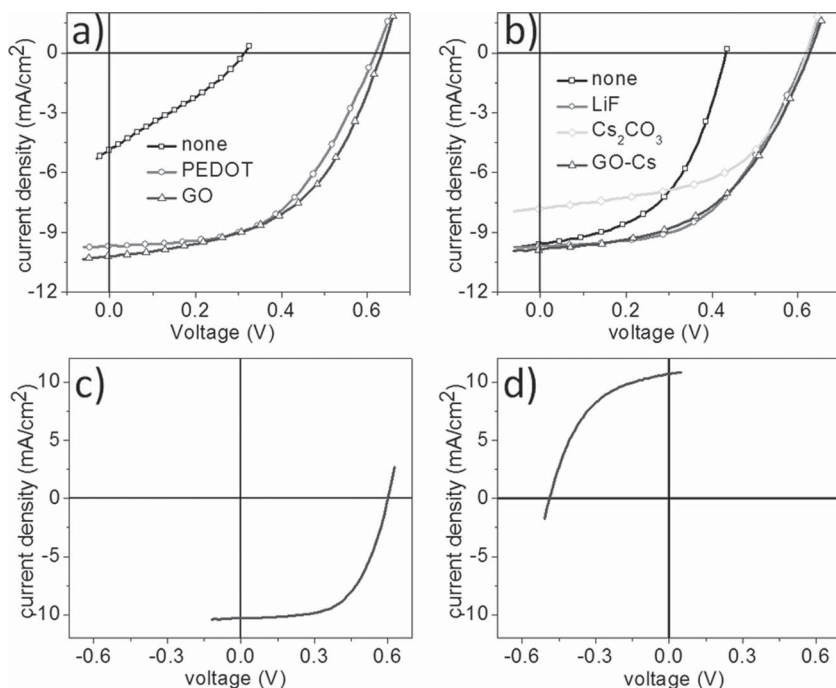


**Figure 3.** a)  $J$ - $V$  curves of devices (ITO/interlayer/P3HT:PCBM/LiF/Al) with different hole-extraction interlayers (Device **A**, **B**, **C**). b)  $J$ - $V$  curves of devices (ITO/PEDOT:PSS/P3HT:PCBM/interlayer/Al) with different electron-extraction interlayers (Device **B**, **D**, **E**, **F**). c)  $J$ - $V$  curve of the normal device with both GO and GO-Cs (i.e., device **G**). d)  $J$ - $V$  curve of the inverted device with both GO and GO-Cs (i.e., device **I**).

extraction performance of GO and GO-Cs are independent of the cathode and anode materials. Therefore, they should be versatile hole-/electron-extraction materials useful for various BHJ solar cells.

In summary, we have demonstrated, for the first time, that simple charge neutralization of the  $-\text{COOH}$  groups in GO with  $\text{Cs}_2\text{CO}_3$  could reverse the charge extraction property in BHJ solar cells. GO can act as an excellent hole-extraction layer while its Cesium-derivative, GO-Cs, is an excellent electron-extraction material for BHJ solar cells, independent of the anode and cathode materials. Their excellent charge extraction performance can be attributed to their unique work functions, coupled with the work function tunability simply through charge neutralization of the periphery  $-\text{COOH}$  groups of GO with  $\text{Cs}_2\text{CO}_3$  into  $\text{COOCs}$  groups, and the ambipolar transporting ability of their basal plane. The normal and inverted devices based on GO hole- and GO-Cs electron-extraction layers both outperform the corresponding standard BHJ solar cells with the state-of-the-art hole- and electron-extraction layers. Therefore, the present study opens new avenues for the design and development of novel charge extraction materials for high-performance solar cells and many other optoelectronic devices.

## Experimental Section

**Synthesis of GO and GO-Cs:** GO was synthesized by the modified Hummer's method published elsewhere.<sup>[13]</sup> To an aqueous solution of GO ( $1.0 \text{ mg mL}^{-1}$ , 40 mL) was added  $\text{Cs}_2\text{CO}_3$  (0.50 g) in several portions. Having been stirred at room temperature ( $20^\circ\text{C}$ ) for 30 min, the solution was filtered through a  $0.2 \mu\text{m}$  PVDF membrane. The solid was then collected, dissolved in water (30 mL), and filtered. The dissolution/filtration process was repeated for two times to afford GO-Cs as a dark solid. Yield: 58 mg.

**Device Fabrication and Measurements:** ITO glass substrates were cleaned sequentially with detergent, deionized water, acetone and isopropanol, followed by drying with  $\text{N}_2$  flow and UV-ozone treatment for 15 min. The interlayers and active layers of the devices were sequentially deposited on the ITO glass using the following spin-coating conditions. The GO layer was spin-coated from its solution in isopropanol ( $0.5 \text{ mg mL}^{-1}$ ) at 2000 rpm for 60 s, followed by heating at  $150^\circ\text{C}$  for 10 min. The GO-Cs layer was spin-coated from its solution in  $\text{H}_2\text{O}/\text{ethanol} = 1/3$  ( $0.5 \text{ mg mL}^{-1}$ ) at 2000 rpm for 60 s, followed by heating at  $150^\circ\text{C}$  for 10 min. PEDOT:PSS layer was spin-coated from the solution (Baytron P VP Al4083 from H. C. Stark, filtered through  $0.45 \mu\text{m}$  PVDF syringe filter) at 5000 rpm for 40 s, followed by heating at  $140^\circ\text{C}$  for 10 min.  $\text{Cs}_2\text{CO}_3$  interlayer was spin-coated from its solution in 2-ethoxyethanol ( $0.4 \text{ mg mL}^{-1}$ ) at 2000 rpm for 60 s, followed by thermal annealing at  $150^\circ\text{C}$  for 10 min. The active layer was spin-coated from the solution of P3HT/PCBM = 1/1 in *o*-dichlorobenzene ( $15 \text{ mg mL}^{-1}$ , filtered with a  $0.2 \mu\text{m}$  PVDF syringe filter) at 700 rpm for 90 s, followed by thermal annealing at  $150^\circ\text{C}$  for 20 min. All the spin-coating processes were carried out at ambient condition. The thickness of the GO, GO-Cs, PEDOT:PSS,  $\text{Cs}_2\text{CO}_3$  and P3HT:PCBM are 2 nm, 2 nm, 30 nm, 2 nm and 200 nm, respectively. After spin-coating of all the organic layers, the devices were transferred to a vacuum chamber for thermal deposition of Al (100 nm) with/without LiF (1 nm) at a pressure of  $10^{-7}$  Torr. The area of each device was  $0.16 \text{ cm}^2$ , as determined by the overlap of the ITO and the evaporated Al. The devices were tested in a  $\text{N}_2$  glovebox using a Keithley 2400 source meter and a Newport Oriel sol 2A solar simulator (300 W). The light intensity was calibrated to be  $100 \text{ mW cm}^{-2}$  using a calibrated Si solar cell, which had been standardized by the National Renewable Energy Laboratory.

## Supporting Information

Supporting Information is available from the Wiley Online Library or from the author.

## Acknowledgements

The authors are very grateful for the financial support from AFOSR under the Polymer Chemistry Task in the Directorate of Chemistry and Life Sciences (Dr. Charles Lee-program Manager). Partial support from NSF-DMR-1106160, Wenzhou Medical College, the Zhejiang Department of Science and Technology (2009C13019), and the Ministry of Science and Technology of China (2009DFB30380) is also acknowledged.

Received: December 27, 2011

Revised: February 1, 2012

Published online:

- [1] K. S. Novoselov, A. K. Geim, S. V. Morozov, D. Jiang, Y. Zhang, S. V. Dubonos, I. V. Grigorieva, A. A. Firsov, *Science* **2004**, 306, 666.
- [2] M. J. Allen, V. C. Tung, R. B. Kaner, *Chem. Rev.* **2010**, 110, 132.
- [3] D. S. Yu, Y. Yang, M. Durstock, J.-B. Baek, L. M. Dai, *ACS Nano* **2010**, 4, 5633.
- [4] D. S. Yu, K. Park, M. Durstock, L. M. Dai, *J. Phys. Chem. Lett.* **2011**, 2, 1113.
- [5] D. Yu, L. Dai, *Appl. Phys. Lett.* **2010**, 96, 143107.
- [6] Y. Liu, D. Yu, C. Zeng, Z. Miao, L. Dai, *Langmuir* **2010**, 26, 6158.
- [7] L. Qu, Y. Liu, J. B. Baek, L. Dai, *ACS Nano* **2010**, 4, 1321.
- [8] X. Xie, L. Qu, C. Zhou, Y. Li, J. Zhu, H. Bai, G. Shi, L. Dai, *ACS Nano* **2010**, 4, 6050.
- [9] C. X. Guo, G. H. Guai, C. M. Li, *Adv. Energy Mater.* **2011**, 1, 448.
- [10] C. X. Guo, X. T. Zheng, Z. S. Lu, X. W. Lou, C. M. Li, *Adv. Mater.* **2010**, 22, 5164.
- [11] G. Eda, M. Chhowalla, *Adv. Mater.* **2010**, 22, 2392.
- [12] D. R. Dreyer, S. Park, C. W. Bielawski, R. S. Ruoff, *Chem. Soc. Rev.* **2010**, 39, 228.
- [13] Y. Xue, H. Chen, D. S. Yu, S. Y. Wang, M. Yardeni, Q. Dai, Y. Liu, J. Qu, L. Dai, *Chem. Commun.* **2011**, 47, 11689.
- [14] D. Yu, E. Negelli, R. Naik, L. Dai, *Angew. Chem. Int. Ed.* **2011**, 50, 6575.
- [15] S.-Y. Bae, I. Y. Jon, Y. Yang, N. Park, H. S. Shin, S. Park, R. S. Ruoff, L. Dai, J.-B. Baek, *ACS Nano* **2011**, 5, 4974.
- [16] G. Yu, J. Gao, J. C. Hummelen, F. Wudl, A. J. Heeger, *Science* **1995**, 270, 1789.
- [17] G. Li, V. Shrotriya, J. Huang, Y. Yao, T. Moriarty, K. Emery, Y. Yang, *Nat. Mater.* **2005**, 4, 864.
- [18] B. C. Thompson, J. M. J. Fréchet, *Angew. Chem. Int. Ed.* **2008**, 47, 58.
- [19] G. Dennler, M. C. Scharber, C. J. Brabec, *Adv. Mater.* **2009**, 21, 1434.
- [20] R. Steim, F. R. Kogler, C. J. Brabec, *J. Mater. Chem.* **2010**, 20, 2499.
- [21] J. H. Park, T.-W. Lee, B.-D. Chin, D. H. Wang, O. O. Park, *Macromol. Rapid Commun.* **2010**, 31, 2095.
- [22] A. Sharma, A. Haldi, W. J. Potscavage Jr., P. J. Hotchkiss, S. R. Marder, B. Kippelen, *J. Mater. Chem.* **2009**, 19, 5298.
- [23] V. Shrotriya, G. Li, Y. Yao, C.-W. Chu, Y. Yang, *Appl. Phys. Lett.* **2006**, 88, 073508.
- [24] M. D. Irwin, D. B. Buchholz, A. W. Hains, R. P. H. Chang, T. J. Marks, *PNAS* **2008**, 105, 2783.
- [25] J. Y. Kim, S. H. Kim, H. H. Lee, K. Lee, W. Ma, X. Gong, A. J. Heeger, *Adv. Mater.* **2006**, 18, 572.
- [26] H.-L. Yip, S. K. Hau, N. S. Baek, H. Ma, A. K.-Y. Jen, *Adv. Mater.* **2008**, 20, 2376.

- [27] T.-Y. Chu, J. Lu, S. Beaupre, Y. Zhang, J.-R. Pouliot, S. Wakim, J. Zhou, M. Leclerc, Z. Li, J. Ding, Y. Tao, *J. Am. Chem. Soc.* **2011**, 133, 4250.
- [28] Z. He, C. Zhong, X. Huang, W.-Y. Wong, H. Wu, L. Chen, S. Su, Y. Cao, *Adv. Mater.* **2011**, 23, 4636.
- [29] T.-Y. Chu, S.-W. Tsang, J. Zhou, P. G. Verly, J. Lu, S. Beaupré, M. Leclerc, Y. Tao, *Sol. Energy Mater. Sol. Cells*, **2012**, 96, 155.
- [30] C. A. Amb, S. Chen, K. R. Graham, J. Subbiah, C. E. Small, F. So, J. R. Reynolds, *J. Am. Chem. Soc.* **2011**, 133, 10062.
- [31] Y. Wang, S. W. Tong, X. F. Xu, B. Özyilmaz, K.-P. Loh, *Adv. Mater.* **2011**, 23, 1514.
- [32] S. Bae, H. Kim, Y. Lee, X. F. Xu, J.-S. Park, Y. Zheng, J. Balakrishnan, Y. Lei, H. R. Kim, Y. I. Song, Y. J. Kim, B. Özyilmaz, J. H. Ahn, B. H. Hong, S. Iijima, *Nat. Nanotechnol.* **2010**, 5, 574.
- [33] V. C. Tung, J.-H. Huang, I. Tevis, F. Kim, J. Y. Kim, C.-W. Chu, S. I. Stupp, J. X. Huang, *J. Am. Chem. Soc.* **2011**, 133, 4940.
- [34] S. Park, J. An, R. D. Piner, I. Jung, D. X. Yang, A. Velemaanni, S. T. Nguyen, R. S. Ruoff, *Chem. Mater.* **2008**, 20, 6592.
- [35] F.-C. Chen, J.-L. Wu, S. S. Yang, K.-H. Hsieh, W.-C. Chen, *J. Appl. Phys.* **2008**, 103, 103721.
- [36] J. S. Huang, Z. Xu, Y. Yang, *Adv. Funct. Mater.* **2007**, 17, 1966.
- [37] Y. Gao, H. L. Yip, S. K. Hau, K. M. O'Malle, N. Cho, H. Z. Chen, A. K. Y. Jen, *Appl. Phys. Lett.* **2010**, 97, 203306.
- [38] Y. Gao, H. L. Yip, K.-S. Chen, K. M. O'Malle, O. Acton, Y. Sun, G. Ting, H. Z. Chen, A. K. Y. Jen, *Adv. Mater.* **2011**, 23, 1903.
- [39] S. S. Li, K. H. Tu, C. C. Lin, C. W. Chen, M. Chhowalla, *ACS Nano* **2010**, 4, 3169.
- [40] S. Wang, P. K. Ang, Z. Q. Wang, A. L. L. Tang, J. T. L. Thong, K. P. Loh, *Nano Lett.* **2010**, 10, 92.